

# HIGH-ENERGY COLLIDING CRYSTALS - A THEORETICAL STUDY\*

Jie Wei<sup>†</sup>, Institute of High Energy Physics, China and Brookhaven National Laboratory, USA  
 Hiromi Okamoto, Hiroshi Sugimoto, Hiroshima University, Japan  
 Yosuke Yuri, Japan Atomic Energy Agency, Japan  
 Andrew Sessler, Lawrence Berkeley National Laboratory, USA

## Abstract

Recent theoretical investigations of beam crystallization using computer modeling based on the method of molecular dynamics (MD) and analytical approach based on the phonon theory [1, 2, 3] are motivated by the study of colliding crystalline beams [4]. Analytical study of crystal stability in an alternating-gradient (AG) focusing ring was previously limited to the smooth approximation. In a typical ring, results obtained under such approximation largely agrees with that obtained with the MD simulation. However, as we explore ring lattices appropriate for beam crystallization at high energies (Lorentz factor  $\gamma$  much larger than the transverse tunes  $\nu_x, \nu_y$ ) [5], this approximation fails. Here, we present a newly developed phonon theory in a time-dependent Hamiltonian system representing the actual AG-focusing ring and predict the stability of 1D crystals at high energies. Luminosity enhancement is illustrated in examples of rare-ion colliders based on ordered 1D strings of ions.

## INTRODUCTION

It is well-known that to create a crystal, two conditions need to be satisfied. First, the storage ring must operate below the transition energy so that the particle motion is in a positive-mass regime. Second, resonances between the oscillations of a crystal and the AG-focusing lattice structure must be avoided so as to prevent heating and thus destruction of the crystal. This requires that the phase advance per lattice period must not exceed  $127^\circ$  (in practice not more than  $90^\circ$  [6, 7]).

In this work, we are motivated by the desire to collide one ion crystal with another or to collide an electron beam with an ion crystal. We desire to do so because in such colliders the usual beam-beam limit can be greatly exceeded. The usual limit is roughly a change in tune,  $\Delta\nu_{bb}$  of less than 0.01, but for a crystal the limit (destruction of the crystal or an ordered avoidance of ions colliding) occurs for  $\Delta\nu_{bb} \sim 1$ . Since the luminosity varies as the square of  $\Delta\nu_{bb}$ , the enhancement is of the order of  $10^4$ .

Colliders are of significant interests at high energies. So, the very first question we want to address is can we make crystals at high energy. We shall show that the answer is positive. Then we go on to explore lattices appropriate for high energy and, in particular, low-momentum-compactness compact lattices where the transverse tunes are

relatively low, i.e.,  $\gamma_T^{-2} \ll \nu_x^{-2}$ . These lattices can not be described by the smooth approximation based on which previous phonon theory was developed [3]. We develop a new formalism appropriate for studying 1D crystal stability in general AG lattices. In comparison, we study both 1D and multi-dimensional high-energy crystals using the MD method. Finally, we present examples of ion-ion and electron-ion colliders with 1D ordered ions.

## COLLIDING-BEAM HAMILTONIAN

The rest-frame motions of particles interacting through the Coulomb fields are governed by the Hamiltonian [8]

$$H = \frac{1}{2} \sum_{\ell} (P_{x,\ell}^2 + P_{y,\ell}^2 + P_{z,\ell}^2) - \sum_{\ell} \gamma x_{\ell} P_{z,\ell} + \frac{1}{2} \sum_{\ell} (\nu_x^2 x_{\ell}^2 + \nu_y^2 y_{\ell}^2) + V_C + V_{bb}, \quad (1)$$

where  $\nu_x$  and  $\nu_y$  are the transverse tunes,  $\gamma$  is the Lorentz factor, and the summation extends over all particles  $l$  in the beam traveling in one direction. In Eq. (1), all canonical variables are scaled as dimensionless by expressing the time,  $t$ , in units of  $\rho/\beta\gamma c$ , the spatial coordinates  $x$ ,  $y$ , and  $z$  in units of the characteristic inter-particle distance  $\xi \equiv (r_0 \rho^2 / \beta^2 \gamma^2)^{1/3}$ , and the energy in units of  $\beta^2 \gamma^2 e^2 / \xi$ , where  $\beta c$  is the velocity of the reference particle,  $r_0$  is its classical radius, and  $\rho$  is the bending radius of the ring under the dipole magnetic field. The Coulomb potential is given by

$$V_C = \frac{1}{2} \sum_{\ell \neq m} \frac{1}{|\mathbf{r}_{\ell} - \mathbf{r}_m|}, \quad (2)$$

where

$$|\mathbf{r}_{\ell} - \mathbf{r}_m| = \left[ (x_{\ell} - x_m)^2 + (y_{\ell} - y_m)^2 + (z_{\ell} - z_m)^2 \right]^{1/2}.$$

Interaction with the colliding beam occurs once per lattice period in a very short time, so it is treated as a lumped kick in momentum. The kick on particle  $l$  can be represented by

$$V_{bb} = \sum_j \frac{(1 + \beta^2) \gamma \xi}{\rho \sqrt{b_{min}^2 + b_{ij}^2}} \quad (3)$$

where  $b_{ij}^2 = (x_i - x_j)^2 + (y_i - y_j)^2$  is the square of the transverse separation and  $b_{min} = (1 + \beta^2) r_0 / (4 \beta^2 \gamma^2 \xi)$  is the minimum separation in the beam rest frame, and the summation,  $j$ , is over all the particles in the opposite beam. We find that if the kick is large comparing with that of the crystalline space charge, then the ground state is two crystals separated in space at the crossing point; i.e. there are

\* Work performed under the auspices of the Chinese Academy of Sciences and the U.S. Department of Energy.

<sup>†</sup> weijie@ihep.ac.cn and jwei@bnl.gov

no overlapping. If, however, the beam-beam effect is not too large then the two crystals do overlap and beam-beam nuclear interactions can occur.

A convenient measure of both the beam-beam and the space-charge forces is given by assuming a uniform charge distribution within the beam. This is usually an underestimate of the actual space-charge and beam-beam forces when the beam is crystallized. Let  $R$  be the average radius of the machine,  $\beta_{xy}^*$  be the  $\beta$  values at the crossing point,  $N_B$  be the number of crossing per revolution,  $N_0$  be the number of ions per bunch,  $\lambda_0$  be the peak number of ions per unit length, and  $a$  be the full transverse radius of the bunch, we have:

$$\Delta\nu_{sc} = \frac{-\lambda_0 R r_0 \beta_{xy}}{\beta^2 \gamma^3 a^2}, \quad \Delta\nu_{bb} = \frac{-N_B N_0 (1 + \beta^2) r_0 \beta_{xy}}{4\pi \beta^2 \gamma a^2} \quad (4)$$

Fig. 1 shows an example of colliding multi-shell crystals obtained by computer simulation based on Eq. 1 using the MD method [4].

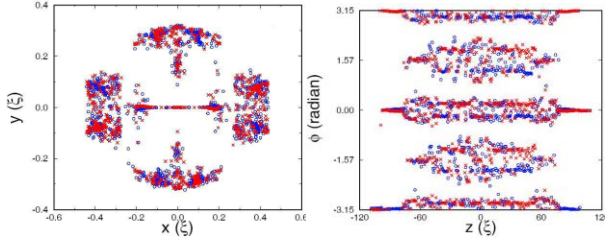


Figure 1: Formation of colliding crystalline beams with 1000 macro particles in each beam. The space charge tune shift  $\Delta\nu_{sc} = -3.8$  and the beam-beam tune shift  $\Delta\nu_{bb} = 0.27$ . The crosses correspond to one beam while the circles correspond to the other.  $\phi$  is the polar angle.

## LATTICE FOR HIGH-ENERGY CRYSTAL

To form crystals at high energy for enhanced luminosity, we explore ring lattices with high ( $\gamma_T \gg \nu_{x,y}$ ) or imaginary ( $\gamma_T^2 < 0$ ) transition energy. A low-momentum-compaction lattice (i.e.,  $\gamma_T^{-2} \ll \nu_x^{-2}$ ) that satisfies the maintenance condition is shown in Fig. 2. The short, negative-bend dipoles at the high-dispersion region compensate for the long, regular dipoles at the low-dispersion region. Such lattice was proposed in 1955 to avoid transition crossing [9]. A variation of the structure was recently proposed for the Fixed Field Alternating Gradient (FFAG) accelerator. The cell phase advance is kept below  $90^\circ$  [10].

## THEORETICAL APPROACHES

Theoretical investigation of crystal stability mainly consists of three methods all based on the beam-rest-frame Hamiltonian. The first is phonon spectrum analysis under the smooth approximation of the machine lattice [3]. The second is generalized phonon spectrum analysis for the actual machine lattice. The third is computer simulation using the MD method for the actual machine lattice.

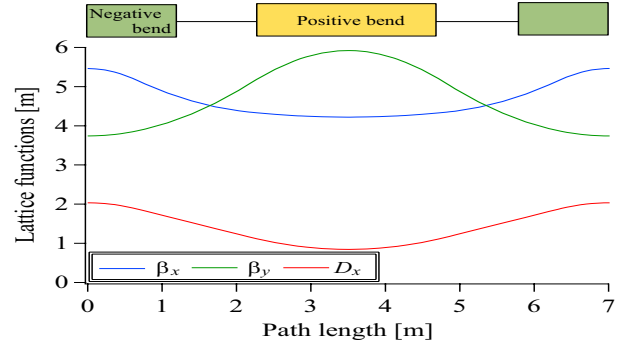


Figure 2: Imaginary- $\gamma_T$  negative-bend lattice with  $87^\circ$  horizontal phase advance. The middle (positive) bend is of combined-function (dipole and defocusing quadrupole).

## Phonon Theory under the Smooth Approximation

The analysis is based on linearized Coulomb forces around the equilibrium positions of the particles. Write the spatial coordinates of  $\ell$ -th ion in a crystalline state as  $(X_\ell, Y_\ell, Z_\ell)$ ,

$$\begin{aligned} x_\ell &= X_\ell + \delta x_\ell, \quad \delta x_\ell = \tilde{x}_\ell \exp[i(\omega t - k Z_\ell)], \\ y_\ell &= Y_\ell + \delta y_\ell, \quad \delta y_\ell = \tilde{y}_\ell \exp[i(\omega t - k Z_\ell)], \\ z_\ell &= Z_\ell + \delta z_\ell, \quad \delta z_\ell = \tilde{z}_\ell \exp[i(\omega t - k Z_\ell)]. \end{aligned} \quad (5)$$

When there are  $N$  particles per unit cell of length  $L$ , we obtain the linearized equations of motion in a storage ring,

$$\omega^2 \tilde{x}_\ell = -i\gamma\omega \tilde{z}_\ell + (\nu_x^2 - \gamma^2) \tilde{x}_\ell + \sum_{n=-\infty}^{\infty} \sum_{m=1}^N \quad (6)$$

$$\left\{ \begin{aligned} & \left[ \frac{1}{R_{\ell mn}^3} - \frac{3(X_\ell - X_m)^2}{R_{\ell mn}^5} \right] \left[ e^{ik(Z_\ell - Z_m - nL)} \tilde{x}_m - \tilde{x}_\ell \right] \\ & - \frac{3(X_\ell - X_m)(Y_\ell - Y_m)}{R_{\ell mn}^5} \left[ e^{ik(Z_\ell - Z_m - nL)} \tilde{y}_m - \tilde{y}_\ell \right] \\ & - \frac{3(X_\ell - X_m)(Z_\ell - Z_m - nL)}{R_{\ell mn}^5} \left[ e^{ik(Z_\ell - Z_m - nL)} \tilde{z}_m - \tilde{z}_\ell \right] \end{aligned} \right\}$$

$$\omega^2 \tilde{y}_\ell = \nu_y^2 \tilde{y}_\ell + \sum_{n=-\infty}^{\infty} \sum_{m=1}^N \quad (7)$$

$$\left\{ \begin{aligned} & - \frac{3(X_\ell - X_m)(Y_\ell - Y_m)}{R_{\ell mn}^5} \left[ e^{ik(Z_\ell - Z_m - nL)} \tilde{x}_m - \tilde{x}_\ell \right] \\ & + \left[ \frac{1}{R_{\ell mn}^3} - \frac{3(Y_\ell - Y_m)^2}{R_{\ell mn}^5} \right] \left[ e^{ik(Z_\ell - Z_m - nL)} \tilde{y}_m - \tilde{y}_\ell \right] \\ & - \frac{3(Y_\ell - Y_m)(Z_\ell - Z_m - nL)}{R_{\ell mn}^5} \left[ e^{ik(Z_\ell - Z_m - nL)} \tilde{z}_m - \tilde{z}_\ell \right] \end{aligned} \right\}$$

$$\omega^2 \tilde{z}_\ell = i\gamma\omega \tilde{x}_\ell + \sum_{n=-\infty}^{\infty} \sum_{m=1}^N \quad (8)$$

$$\left\{ \begin{aligned} & - \frac{3(X_\ell - X_m)(Z_\ell - Z_m - nL)}{R_{\ell mn}^5} \left[ e^{ik(Z_\ell - Z_m - nL)} \tilde{x}_m - \tilde{x}_\ell \right] \\ & - \frac{3(Y_\ell - Y_m)(Z_\ell - Z_m - nL)}{R_{\ell mn}^5} \left[ e^{ik(Z_\ell - Z_m - nL)} \tilde{y}_m - \tilde{y}_\ell \right] \\ & + \left[ \frac{1}{R_{\ell mn}^3} - \frac{3(Z_\ell - Z_m - nL)^2}{R_{\ell mn}^5} \right] \left[ e^{ik(Z_\ell - Z_m - nL)} \tilde{z}_m - \tilde{z}_\ell \right] \end{aligned} \right\}$$

where

$$R_{\ell mn} = \sqrt{(X_\ell - X_m)^2 + (Y_\ell - Y_m)^2 + (Z_\ell - Z_m - nL)^2}$$
 $\ell = 1, \dots, N$ , and  $R_{\ell mn} = 0$  term is excluded from the double sum. A computer algorithm was developed to obtain the eigenvalues of the system for a general crystalline structure beyond 1D. Practically, systems of up to  $N = 50$  particles per MD supercell were studied.

For 1D crystals,  $N = 1$ , Eqs. 6, 7, and 8 can be solved analytically. The phonon bands are calculated as

$$\begin{aligned} \omega_1^2 &= \frac{1}{2} \left\{ \nu_x^2 + \Omega^2 + \sqrt{(\nu_x^2 + \Omega^2)^2 - 8\Omega^2(\nu_x^2 - \gamma^2 - \Omega^2)} \right\} \\ \omega_2^2 &= \nu_y^2 - \Omega^2 \\ \omega_3^2 &= \frac{1}{2} \left\{ \nu_x^2 + \Omega^2 - \sqrt{(\nu_x^2 + \Omega^2)^2 - 8\Omega^2(\nu_x^2 - \gamma^2 - \Omega^2)} \right\} \end{aligned} \quad (9)$$

where

$$\Omega^2 = 2 \sum_{n=1}^{\infty} \frac{1 - \cos(kn/\Lambda)}{(n/\Lambda)^3} \geq 0 \quad (10)$$

with  $\Lambda$  being the scaled dimensionless line density defined by  $\Lambda = N/L$ , and the wave number  $k$  varies from  $-\pi\Lambda$  to  $\pi\Lambda$ . The actual line density  $\lambda$  in the laboratory frame can be related to  $\Lambda$  as  $\lambda = \Lambda/(\gamma\xi)$ . The 1D structure is stable if all the eigenvalues are real for any  $k$ .

Fig. 3 shows the stability of 1D crystalline beams at different line densities as functions of the beam energy. Stable 1D structure exists for energies up to a threshold  $\gamma_{th}$  corresponding to the transition energy of the machine, i.e.,  $\gamma_{th} = \gamma_T = \nu_x$ . For energies below transition ( $\gamma < \gamma_{th}$ ), there exists a threshold density beyond which the crystalline structure is beyond 1D.

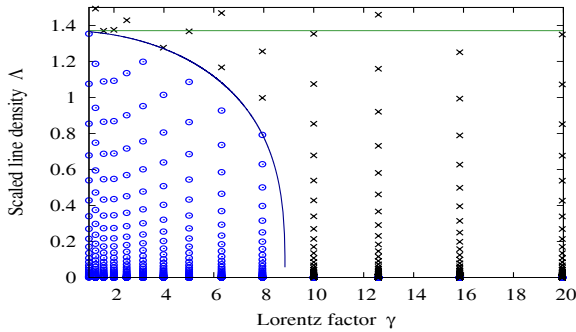


Figure 3: Stable region (blue circles) of 1D crystals evaluated using the smooth approximation. The transverse tunes are  $\nu_x = \nu_y = 8.85$ . The threshold energy corresponds to  $\gamma_{th} = \gamma_T = 8.85$  beyond which no crystals are predicted.

### Phonon Theory for a General Lattice

The smooth approximation with  $\gamma_T = \nu_x$  fails to describe features of machine lattices where the transition energy is either high ( $\gamma_T \gg \nu_x$ ) or imaginary. We hereby develop the phonon theory applicable to a general machine lattice where  $\gamma_T$  may deviate significantly from  $\nu_x$  and  $\nu_y$ .

Divide the machine into sections along the circumference; within each section the external force (i.e. magnetic

focusing and bending) is constant. The one-turn transfer  $M$  is the product of the transfer matrices across each section  $i$ ,

$$M = \prod_{i=1}^{N_{lat}} M_i \quad (11)$$

where  $N_{lat}$  is the number of sections along the machine. In the case of a 1D crystal under regular bending and focusing forces, the vertical motion ( $y$ ) is decoupled from the motion in the other two directions ( $x, z$ ). The one-turn transfer matrices in  $y$  and  $x, z$  are

$$M_y = \prod_{i=1}^{N_{lat}} M_{y,i}, \quad M_{xz} = \prod_{i=1}^{N_{lat}} M_{xz,i} \quad (12)$$

Within each section, the transfer matrices may be obtained by linearizing the Coulomb forces around the equilibrium positions of the particles,

$$M_{y,i} = \begin{bmatrix} \cos \omega_{2i} t_i & \frac{\sin \omega_{2i} t_i}{\omega_{2i}} \\ -\omega_{2i} \sin \omega_{2i} t_i & \cos \omega_{2i} t_i \end{bmatrix} \quad (13)$$

and

$$M_{xz,i} = \bar{M}_{xz,i} \bar{M}_{xz,i}^{-1}(0) \quad (14)$$

where

$$\bar{M}_{xz,i} = \begin{bmatrix} \bar{M}_{xz,i}^{11} & \bar{M}_{xz,i}^{12} \\ \bar{M}_{xz,i}^{21} & \bar{M}_{xz,i}^{22} \end{bmatrix} \quad (15)$$

with the sub-matrices given by

$$\bar{M}_{xz,i}^{11} = \begin{bmatrix} e^{i\omega_{1i} t_i} & e^{-i\omega_{1i} t_i} \\ i\omega_{1i} t_i e^{i\omega_{1i} t_i} & -i\omega_{1i} t_i e^{-i\omega_{1i} t_i} \end{bmatrix} \quad (16)$$

$$\bar{M}_{xz,i}^{12} = \begin{bmatrix} e^{i\omega_{3i} t_i} & e^{-i\omega_{3i} t_i} \\ i\omega_{3i} t_i e^{i\omega_{3i} t_i} & -i\omega_{3i} t_i e^{-i\omega_{3i} t_i} \end{bmatrix} \quad (17)$$

$$\bar{M}_{xz,i}^{21} = \begin{bmatrix} c_{31} e^{i\omega_{1i} t_i} & -c_{31} e^{-i\omega_{1i} t_i} \\ c_{41} e^{i\omega_{1i} t_i} & c_{41} e^{-i\omega_{1i} t_i} \end{bmatrix} \quad (18)$$

$$\bar{M}_{xz,i}^{22} = \begin{bmatrix} c_{33} e^{i\omega_{3i} t_i} & -c_{33} e^{-i\omega_{3i} t_i} \\ c_{43} e^{i\omega_{3i} t_i} & c_{43} e^{-i\omega_{3i} t_i} \end{bmatrix} \quad (19)$$

and

$$\bar{M}_{xz,i}(0) = \begin{bmatrix} 1 & 1 & 1 & 1 \\ i\omega_{1i} t_i & -i\omega_{1i} t_i & i\omega_{3i} t_i & -i\omega_{3i} t_i \\ c_{31} & -c_{31} & c_{33} & -c_{33} \\ c_{41} & c_{41} & c_{43} & c_{43} \end{bmatrix} \quad (20)$$

where the coefficients are given by

$$c_{3n} = \frac{i\omega_{ni}\gamma}{\omega_{ni}^2 - 2\Omega^2}, \quad c_{4n} = \frac{-2\Omega^2\gamma}{\omega_{ni}^2 - 2\Omega^2}, \quad n = 1, 3 \quad (21)$$

with  $\omega_{ni}$  in each section  $i$  given by

$$\begin{aligned} \omega_{1i}^2 &= \frac{1}{2} \left\{ \nu_{xi}^2 + \Omega^2 + \sqrt{(\nu_{xi}^2 + \Omega^2)^2 - 8\Omega^2(\nu_{xi}^2 - \gamma^2 - \Omega^2)} \right\} \\ \omega_{2i}^2 &= \nu_{yi}^2 - \Omega^2 \\ \omega_{3i}^2 &= \frac{1}{2} \left\{ \nu_{xi}^2 + \Omega^2 - \sqrt{(\nu_{xi}^2 + \Omega^2)^2 - 8\Omega^2(\nu_{xi}^2 - \gamma^2 - \Omega^2)} \right\} \end{aligned} \quad (22)$$

where  $\Omega^2$  is given by Eq. 10. The 1D crystalline structure is defined to be stable if all the eigenvalues of the one-turn matrix (Eq. 11) are real for any wave number  $k$ .

Fig. 4 shows the stability of the 1D crystalline beams in a high-transition lattice with  $\gamma_T = 105$  much higher than the transverse tunes ( $\nu_x = \nu_y = 8.85$ ). At low energy,

$\gamma < \nu_x$ , the stable region is similar to that predicted by the phonon theory using the smooth approximation (Fig. 3). However, at energies beyond ( $\gamma > \nu_x$ ) stable 1D structures are also predicted, although the threshold density decreases with energy. A narrow stable region exists even when the energy is above transition ( $\gamma > \gamma_T$ ).

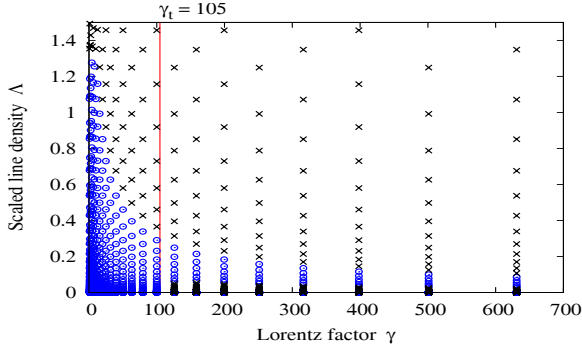


Figure 4: Stable region (blue circles) of 1D crystals evaluated with the phonon theory based on the actual lattice. The ring consists of 36 lattice periods each containing four uniform-external-force sections as illustrated in Fig. 2. Here,  $\nu_x = \nu_y = 8.85$ , and  $\gamma_T = 105$ .

### Molecular Dynamics Method

Using the MD method [1, 2], Fig. 5 shows the region where crystalline structures are obtained in the high-transition lattice ( $\gamma_T = 105$ ,  $\nu_x = \nu_y = 8.85$ ). At energies up to  $\gamma \approx \nu_{x,y}$ , stable crystals from 1D string to 3D multi-shell are formed depending on the line density of the beam, as shown in Fig. 6. Formation of stable 3D crystals becomes increasingly difficult for higher beam energies. At  $\gamma = 20$ , only 2D crystals are formed. Due to reduction of the effective horizontal focusing [3], the zig-zag structure extends in the horizontal plane. Stable 1D structures are obtained at energies up to the transition but not beyond.

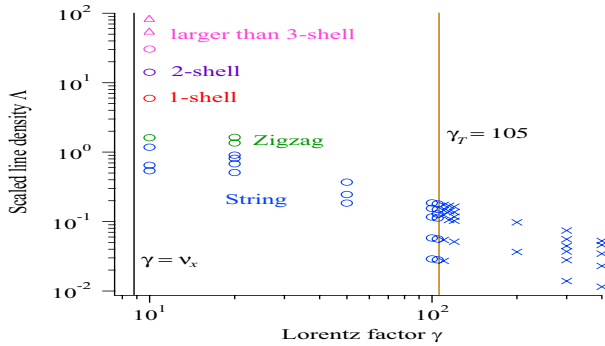


Figure 5: Stable region (non-crosses) of 1D, 2D, and 3D crystals evaluated using the MD method for the high-transition lattice. The machine lattice is the same as that used for Fig. 4 with  $\nu_x = \nu_y = 8.85$ , and  $\gamma_T = 105$ .

MD simulations are also used to study the crystal formation in an imaginary- $\gamma_T$  lattice. Lattice functions of a ring lattice period is shown in Fig. 2. The phase advances per

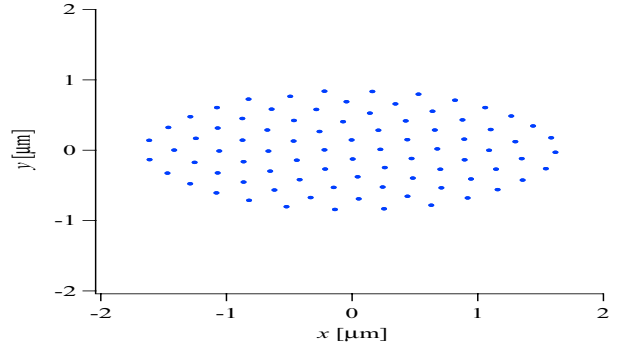


Figure 6: A multi-shell crystalline beam of  $^{24}\text{Mg}^+$  ions formed with the high-transition ( $\gamma_T = 105$ ,  $\nu_x = \nu_y = 8.85$ ) lattice at the energy corresponding to  $\gamma = 10$  and density of  $6.2 \times 10^9/\text{m}$  in the laboratory frame. During simulation, both the transverse and tapered cooling are applied [11]. If a crystalline state is reached, the cooling force is removed to test the stability of the formed crystal.

lattice period are  $\mu_x = \mu_y = 87^\circ$ . Fig. 7 shows the region where crystalline structures are obtained. Again, at energies up to  $\gamma \approx \nu_{x,y}$ , stable crystals from 1D string to 3D multi-shell are formed depending on the line density of the beam. Formation of stable 3D crystals becomes increasingly difficult for higher beam energies. On the other hand, stable 1D structures are obtained at very high energies.

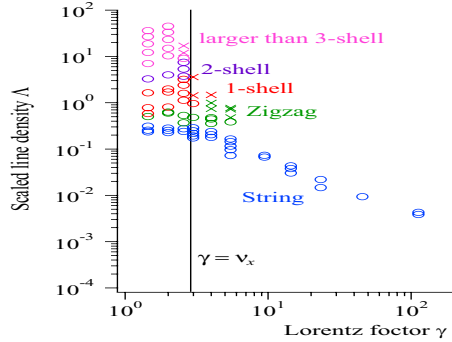


Figure 7: Stable region (non-crosses) of 1D, 2D, and 3D crystals evaluated using the MD method for the imaginary-transition lattice. The transverse tunes are  $\nu_x = \nu_y = 2.90$ . The transition energy corresponds to  $\gamma_T = i13$ . The machine of 84 m circumference consists of 12 lattice periods.

## COLLIDING CRYSTALS

We provide two examples using 1D ordered ion beams in a collider to achieve significant luminosity with a small number of ions.

### Rare-ion Collider with Ordered Ions

We adopt the main machine parameters of the Relativistic Heavy Ion Collider (RHIC) to illustrate the performance of a rare-ion collider with two counter-circulating beams of 360 bunches each containing  $4 \times 10^6$  ions. At the beam energy of  $\gamma = 20$  below transition, the characteristic distance

in the rest frame is  $\xi = 19 \mu\text{m}$ . For the beam to be an ordered 1D string, the line density in the laboratory frame must be below  $\Lambda_{\text{th}}\gamma/\xi$  where

$$\Lambda_{\text{th}} = 0.62\nu_{eff}^{2/3}, \quad \nu_{eff}^2 = \min(\nu_x^2 - \gamma^2, \nu_y^2) \quad (23)$$

and the amplitude  $\sigma_{x,y}$  of the transverse motion must be much smaller than the distance between the ions in the rest frame. The luminosity is given by

$$L = \frac{f_0 N_B N_0^2}{4\pi\sigma_{x,y}^*} \quad (24)$$

where  $f_0 = \beta c/2\pi R$ . Under sufficient beam cooling, Table 1 shows that significant luminosity can be attained.

With relatively few number of particles and significant luminosity, the lifetime of the beam is usual short due to the event of collisions. Fast beam cooling like optical-frequency-range stochastic cooling and high-energy electron cooling is necessary. Ref. [12] indicates that with efficient beam cooling, the ordered state can be maintained in the presence of significant event rate.

### Electron-ion Collider with Ordered Ions

Following the example presented in Ref. [13], significant luminosity can be achieved when a beam of rare ions formed as 1D ordered string collides with an electron beam of similar beam radius (Table 2) [13, 14]. Electron cooling is proposed to cool the ion beam to an ordered state.

## SUMMARY AND DISCUSSIONS

For regular machine lattices, multi-shell crystals can be formed for energies ( $\gamma$ ) up to the machine tunes ( $\gamma_{th} \approx \nu_{x,y}$ ). Special lattices can be designed – they are AG-focusing, low-momentum-compactness lattices that have very high or even imaginary transition energy. Thus, it is not necessary to make very large rings to achieve high-energy crystals.

We have developed a phonon formalism for analyzing 1D crystals in such AG-focusing lattices. Stability analysis based on this formalism is compared with the MD

Table 1: Major parameters of a rare-ion collider with ordered ions.

Ring circumference, $2\pi R$ [m]	3834
Ring transition energy, $\gamma_T$	23
Ring transverse tunes, $\nu_x, \nu_y$	29.18, 28.19
Ion charge $Z$ , mass number $A$	79, 197
Ion beam energy, $\gamma$	20
Number of bunches in each ring, $N_B$	360
Bunch length in laboratory frame [m]	1
Number of ions per bunch, $N_0$	$10^6$
Transverse amplitude (ave.), $\sigma_{x,y}$ [m]	$10^{-6}$
Transverse amplitude at IR, $\sigma_{x,y}^*$ [m]	$0.22 \times 10^{-6}$
Momentum spread, $\Delta p/p$	$0.9 \times 10^{-6}$
Inc. space-charge tune shift, $\Delta\nu_{sc}$	-19.5
Beam-beam tune shift, $\Delta\nu_{bb}$	-4.1
Instan. luminosity, $L$ [ $\text{cm}^{-1}\text{s}^{-1}$ ]	$4.7 \times 10^{27}$

Table 2: Major parameters of an electron-ion collider with ordered ions [13].

Ring circumference [m]	108
Ion charge $Z$ , mass number $A$	82, 208
Ion kinetic energy [MeV/n]	180
Total Number of ions in the ring	$3 \times 10^6$
Interaction region length [m]	1
Tran. amplitude at IR [m]	$6 \times 10^{-6}$
Momentum spread, $\Delta p/p$	$1.3 \times 10^{-6}$
Inc. space charge tune shift	-0.25
Beam-beam parameter	1
Instan. luminosity [ $\text{cm}^{-1}\text{s}^{-1}$ ]	$1.4 \times 10^{27}$

simulations. In such lattices, lower-density crystals can be formed at energies much higher than the machine tunes ( $\gamma_{th} \gg \nu_{x,y}$ ). In particular, 1D crystals can be formed in low-momentum-compactness lattices even if  $\gamma \gg \nu_{x,y}$ . However, we find that it is impossible to form multi-shell crystals in this energy regime possibly due to the sensitivity of the effective momentum compaction to the transverse force between the particles.

Even 1D crystals, when made to collide, would have a very interesting luminosity. We have presented two examples of such rare-ion colliders. Performance of an ion-ion collider may be demonstrated by implementing a trap with a storage ring and force the ordered beam in the ring to interact with the crystal formed in the trap.

We thank X.-P. Li, S. Machida, D. Moehl, and D. Trbojevic for helpful discussions. One of the authors (JW) is grateful to M. Steck, D. Moehl and the COOL07 organizing committee for the invitation and support to the workshop.

## REFERENCES

- [1] J. Wei, X.-P. Li, and A. M. Sessler, Phys. Rev. Lett., **73** (1994) 3089
- [2] J. Wei, H. Okamoto, and A.M. Sessler, Phys. Rev. Lett., **80** (1998) 2606
- [3] X.-P. Li, H. Enokizono, H. Okamoto, Y. Yuri, A.M. Sessler, and J. Wei, Phys. Rev. ST-AB, **9** (2006) 034201
- [4] J. Wei, A.M. Sessler, EPAC (1998) 862
- [5] J. Wei, H. Okamoto, S. Ochi et al, EPAC (2006) 2841
- [6] K. Okabe, H. Okamoto, Jpn. J. Appl. Phys. **42** (2003) 4584
- [7] I. Hofmann, L. Laslett, L. Smith, and I. Haber, Part. Accel. **13** (1983) 145
- [8] J. Wei, X.-P. Li, and A.M. Sessler, Proc. 6th Adv. Accel. Conf. (1994) 224
- [9] V.V. Vladimirski, E.K. Tarasov, Theoretical problems of the ring accelerators, USSR Academy of Science (1955)
- [10] C. Johnstone, E. Keil, and D. Trbojevic, private communications
- [11] H. Okamoto, J. Wei, Phys. Rev. E, **58** (1998) 3817
- [12] J. Wei, A.M. Sessler, EPAC (1996) 1179
- [13] T. Katayama, D. Moehl, RIKEN Report (2002)
- [14] I. Meshkov, A. Sidorin, A. Smirnov, E. Syresin, and T. Katayama, Inst. of Phys. & Chem. Res. (RIKEN) Report: RIKEN-AF-AC-34 (2002)